

NASA Technical Paper 1546



Influence of Coolant Tube Curvature on Film Cooling Effectiveness as Detected by Infrared Imagery

S. Stephen Papell, Robert W. Graham,
and Richard P. Cageao

NOVEMBER 1979





NASA Technical Paper 1546

Influence of Coolant Tube Curvature on Film Cooling Effectiveness as Detected by Infrared Imagery

S. Stephen Papell, Robert W. Graham,
and Richard P. Cageao
*Lewis Research Center
Cleveland, Ohio*



National Aeronautics
and Space Administration

**Scientific and Technical
Information Branch**

1979

SUMMARY

Reported herein are thermal film-cooling footprints observed by infrared imagery from straight, curved, and looped coolant tube geometries. It was hypothesized that the differences in secondary flow and in the turbulence structure of flow through these three tubes should influence the mixing behavior of the coolant and the main stream. The coolant was injected across an adiabatic plate through a hole angled at 30° to the surface and in line with the free-stream flow. The data cover a range of blowing rates (mass flow per unit area of coolant divided by free-stream flow from 0.37 to 1.25. The average temperature difference between coolant and tunnel air was 25° C.

Data comparisons confirmed that coolant-tube curvature significantly influences the effectiveness of film cooling. At the blowing rates of 0.37 to 0.54, the curved coolant tube was more effective than the straight tube by as much as 16 to 27 percent. At higher blowing rates (0.82 and 1.25), the curved tube was less effective by as much as 13 to 19 percent. This reversal in data trend occurred at a blowing rate of about 0.70. The film-cooling performance of the looped tube was inferior to both straight and curved tubes at all blowing rates.

INTRODUCTION

The film-cooling mechanism is the injection of a cool film of air into a boundary layer to provide an insulating layer between a hot gas and metal walls. The effectiveness of this film is determined in part by the rate that the coolant mixes with the free-stream boundary layer and the free stream itself. Coolant effectiveness in surface protection, then, depends on the minimization of its dispersion into the free stream and on its adherence to the wall or boundary-layer region. The flow pattern and turbulence structure of the coolant gas should be influential in controlling this mixing process.

Studies of curved channels and pipes have verified that the internal turbulence structure is sensitive to curvature: (a) concave wall increases turbulence level, heat transfer, and friction; (b) convex wall reduces turbulence, heat transfer, and friction. For example, the wall friction and heat transfer of the concave surface of a curved channel are significantly greater than the convex surface (ref. 1). For the particular geometry of reference 1, the differences between the two surfaces appeared to maximize at turning angles beyond 100° and then decrease beyond 165° of turning. Similar trends in heat transfer were observed for gaseous hydrogen flowing in curved tubes (ref. 2).

It is proposed that this apparent difference in the structure of the flow between the convex and concave surfaces of a curved tube should influence the mixing properties of a coolant stream emerging from such a curved tube. If it is possible to admit the stabilized boundary layer of the convex curvature at the downstream edge of the coolant hole, improved adherence of that portion of the coolant to the wall might be realized. The purpose of this investigation then was to examine this hypothesis. If proved correct, this information could be used to obtain more effective protection for turbine blades and vanes.

A flow visualization tunnel and test plate with one coolant hole (used in a previous film cooling study (ref. 3)), was selected for the study. Under the test conditions of reference 3 it had been established that the boundary-layer thickness at the coolant hole was about twice the diameter of the coolant tube, which is at the low end of the scaling range of practical interest. The typical range of boundary-layer-thickness-to-hole-diameter ratio is 2 to 10.

Using the flat-plate turbulent boundary-layer equation from (ref. 4), under test conditions of the present study, the boundary-layer thickness was calculated to be approximately three times the coolant-tube diameter, which, again, is in the scaling range of practical interest.

Reported herein are the thermal film-cooling footprints observed by infrared imagery from straight, curved, and looped coolant-tube geometries. For each case the discharge angle of the coolant was 30° from the wall and in line with free-stream flow. The data cover a range of blowing rates (mass flow per unit area of coolant divided by free-stream flow) from 0.37 to 1.25. The average temperature difference between the coolant and the tunnel air was 25° C.

SYMBOLS

A	area
D	coolant-tube diameter
M	blowing rate, $(\rho V)_c/(\rho V)_\infty$
T	temperature
V	velocity
x	distance from edge of coolant hole
x/D	dimensionless distance
η	adiabatic film cooling effectiveness, $(T_\infty - T_{aw})/(T_\infty - T_c)$
ρ	density

Subscripts:

aw	adiabatic wall
c	coolant
∞	free stream or tunnel air

DESCRIPTION OF APPARATUS

Figure 1 is a schematic drawing of the test setup. The principal components are (a) the flow-visualization tunnel, (b) an infrared camera and detector, and (c) a Hilsch tube for coolant-air supply.

Tunnel

The tunnel is made up of four rectangular sections having a flow area cross section of 15 by 38 centimeters, a contoured inlet, and a transition piece that connects the tunnel to the altitude exhaust system of the laboratory. Three of the rectangular sections are made of transparent plastic. The fourth section, containing the test plate, is made of wood except for one plastic sidewall.

The four rectangular sections can be arranged in any order, so that the developing boundary layer has from a few centimeters to almost 3 meters of development length. For this investigation there was approximately 2 meters of tunnel length (not including the inlet) in front of the coolant hole of the test section. The cooling effectiveness of a single film-cooling tube was observed throughout the test program. The coolant injection angle was inclined 30° with respect to the horizontal, and the plane of inclination was along the flow axis of the tunnel. The wooden floor of the test section, 1.9 centimeters thick with an insulation backing, was assumed to be adiabatic.

Coolant-Tube Configurations

The coolant-tube configurations of this investigation were made of copper tubing with an inside diameter of 1.15 centimeters. The three inlet geometries are shown in figure 2. The conventional straight-tube entry is the reference, and the two curved geometries are the innovations of this investigation. Figure 3 shows the curved tube mated with the test plate. From what is known about curved tubes, or channels, the single bend of approximately 150° should be a near-optimum geometry for observing the possible benefits of curvature in this test section.

In the looped tube, separation and increased friction act on the wall boundary layers to contribute significant losses to the discharging coolant flow. The differences in heat transfer, friction, and turbulence for the convex and concave walls of curved tubes maximize early in the turning (on the order of 90°) and tend to wash out at turning angles beyond 165° . Thus, it was expected that the looped tube would tend to incite more turbulence in the coolant flow and promote mixing with the free stream which would reduce film-cooling effectiveness.

Infrared Camera Equipment

The infrared camera and detector unit is capable of operating in the temperature range -30° to 200° C and can discriminate temperature differences as small as 0.2° C on the surface it is observing. The detector element is indium antimonide cooled by a liquid-nitrogen bath. The detector displays a maximum of two isotherm images on the cathode-ray screen at once. To calibrate the system, one of the isotherms observed was at room temperature, which was the adiabatic temperature of the test plate without film cooling. The associated magnitude of the room temperature was indicated in thermal scale units along the abscissa of the cathode-ray screen. With this room temperature scale as a reference, it was possible to compute all other isotherms observed on the plate. Figure 4 is a pair of isotherm photographs. The two ticks on the bottom scale of figure 4(a) represent an isotherm wall temperature of 19.4° C and the room-temperature reference of 25.8° C. The wall temperature isotherm is displayed as a single line between the two horizontal parallel lines. The reference room-temperature isotherm is displayed as two parallel lines and as the half circle on the upper part of the right vertical line. The two vertical lines are the field of view limits of the infrared detector. Figure 4(b) shows the change in the wall isotherm trace at a higher temperature. For a given test condition about six isotherms were photographed to give a composite picture of the footprint.

As shown in figure 1 radiation absorption was minimized by using a thin plastic film stretched over a window cut into a wooden test section cover plate. A small circular window located over a surface area not influenced by the coolant stream was used to obtain the room air reference isotherm.

Coolant-Air Supply

A very adaptable and convenient method for supplying cooling air appreciably below room temperature was the use of a Hilsch tube. This device, which incorporates a vortex generator element, separates the inlet air into hot- and cold-air streams. This

comes about from the forced vortex or wheel-type angular velocity imparted to the air introduced into the device. Conservation of total energy of the inner portion of the forced vortex causes heat to be transferred to the outer region. Consequently, a relatively cold, inner core of air and a warm, outer ring of air are formed. In the Hilsch tube design the warm- and cold-air discharge ports are on opposite sides of the device. It was found that temperatures of 0° C could be reached quite easily, so this coolant temperature was selected for all of the tests.

The coolant temperature was measured by a thermocouple mounted on the outer wall of each coolant inlet tube. The coolant flow rate was measured by a turbine flowmeter installed between the Hilsch tube and the coolant tube.

EXPERIMENTAL PROCEDURE AND DATA REDUCTION

The controlled parameters for these tests were tunnel velocity, coolant velocity, and coolant temperature (set at 0° C). The tunnel temperature, depending on ambient conditions, was about 25° C. Variations in blowing rate M were obtained by controlling the tunnel and Hilsch-tube airflow values.

After establishing a required blowing rate, the tunnel was run for 45 minutes to obtain steady-state conditions. The infrared camera then photographed a series of isotherms representing the film-cooling-effectiveness footprint. The testing procedure was used for all blowing rates and coolant-tube configurations.

Comparable data were obtained at blowing rates of 0.37, 0.46, 0.54, 0.82, and 1.25. Although the tunnel Reynolds number was varied to set the blowing rates, checks were made to assure that the Reynolds number range covered did not influence the data. The isotherm information was then digitized, converted to engineering units, and plotted. The isotherm traces were identified on the plots in terms of an adiabatic wall film-cooling effectiveness defined as:

$$\eta = \frac{T_{\infty} - T_{aw}}{T_{\infty} - T_c}$$

where T_{∞} , T_c , and T_{aw} are temperatures of the tunnel, coolant, and wall, respectively.

Examples of this data reduction are the full scale computer plots shown on figure 5. Information gleaned from these figures include actual measurements of isotherm temperatures and interpretations of isotherm shapes with regard to the mixing process of the two streams.

Two types of measurements were made from these figures: The first was the centerline length of each isotherm measured from the edge of the coolant-injection hole. The second, made with a planimeter, was the surface area enclosed by the isotherms.

PRESENTATION AND DISCUSSION OF DATA

Centerline Effectiveness Comparisons

The centerline film-cooling-effectiveness data, obtained by measuring the length of each isotherm, are presented in figure 6 for the three coolant-tube configurations. The individual curves represent averaged values of basic data that lie within a ± 0.03 error band as shown in figure 6(b). The data are plotted as film-cooling effectiveness at some dimensionless distance from the edge of the coolant-injection hole. Each figure shows the performance of the three inlet configurations for a particular blowing rate and tunnel velocity.

Significant observations made from these figures include the effectiveness level of the curves relative to each other and, for the higher blowing rates (figs. 6(c) to (e)), the difference in slope of the curves within 2 to 4 diameters of the coolant-injection hole. At these blowing rates, the boundary layer is subject to separation just downstream of the hole, resulting in higher local surface temperatures. This flow separation phenomenon is also depicted in figure 5(b) where four of the isotherm traces close on themselves near the hole.

Figure 6 also shows that the effectiveness data trends for the straight and curved tubes are a function of blowing rate. The centerline cooling effectiveness data presented in figures 6(a) and (b) for the lower blowing rates ($M = 0.37$ and 0.46) show the superior performance of the curved tube over the straight tube. In figure 6(a) the greater effectiveness due to inlet curvature is significant down to about 8 diameters from the edge of the hole. In figure 6(b) this greater effectiveness is observed over the entire length of the film-cooling footprint.

As the blowing rate is increased to 0.54 (fig. 6(c)), a reversal in trend occurs within about $3\frac{1}{2}$ diameters from the hole, although farther downstream the curved tube performance is once again better.

This change in trend persists at the higher blowing rates of 0.82 and 1.25 (as shown on figs. 6(d) and (e)) where the film-cooling effectiveness of the straight-tube is greater than that of the curved tube over the entire footprint, with the largest difference occurring near the coolant-injection hole.

Figure 6 also shows that in all cases the film-cooling effectiveness of the looped tube was lower than both the straight or curved tubes. Although this inferior perfor-

mance of the looped tube was expected, it was not expected that this type of inlet geometry could influence the flow separation phenomena as previously described. Figures 6(c) to (e) show no evidence of boundary-layer separation near the coolant-injection hole for the looped tube data, but considerable separation for both the straight and curved tubes.

Isotherm Surface Area Comparison

Figure 7 illustrates the difference in cooled surface areas obtained with straight and curved tubes under identical test conditions. Equal temperature isotherms are shown in terms of an effectiveness value of 0.46 for a blowing rate of 0.46. It is apparent that a significant increase in film-cooling coverage would occur by use of curved tubes under the conditions described above.

Figure 8 presents comparisons of the straight and curved tubes with isotherm area measurements of the basic data. (The looped tube data, being consistently below the other two configurations, will not be included in the remaining comparisons.) In each plot the surface coverage of each isotherm area is plotted in terms of the film-cooling-effectiveness parameter for a particular blowing rate and tunnel velocity. The individual curves represent averaged values of the basic data. An examination of the figures reveals trends similar to those found with the centerline film-cooling effectiveness data:

The curved tube's cooling effectiveness is clearly superior at the lower blowing rates of 0.37, 0.46, and 0.54 (figs. 8(a) to (c)). The surface area cooled by the curved tube was greater than that of the straight tube, and was greatest at a blowing rate of 0.46. At the higher blowing rates of 0.82 and 1.25 (figs. 8(d) and (e)) the trend reverses; that is, the performance of the straight tube is superior.

Figure 9 shows the percent change in film-cooling effectiveness caused by coolant-tube curvature. The differences in film cooling effectiveness between the straight and curved tube were obtained from figure 8 for isotherm areas of 4 and 16 square centimeters. The percent change in effectiveness plotted as a function of blowing rate (fig. 9) illustrates the reversal in trend that occurs at a blowing rate of about 0.70. At the lower blowing rates the increased performance of the curved tube over the straight tube varies by as much as 16 to 27 percent. At the higher blowing rates the decrease in performance of the curved tube varies by as much as 13 to 19 percent.

CONCLUSIONS

From what is known about turbulent flow in a curved channel, it was hypothesized that improved film cooling could be realized by using a sharply curved coolant tube. This was confirmed for the lower blowing rates of 0.37, 0.46, and 0.54 where the effec-

tiveness of the curved tube was substantially higher than that of the straight tube. In addition, the surface area bounded by a given effectiveness ratio was always greater for the curved tube within this blowing range.

At the higher blowing rates (0.82 and 1.25) the straight coolant tube exhibited superior overall effectiveness. There appears to be a crossover in performance of the two coolant-tube geometries at a blowing rate of approximately 0.70. Without detailed internal flow information on the turbulence and velocity profiles for the straight and curved tubes, an explanation of this crossover is not available. For practical applications of film cooling, the lower blowing rates (<0.7) are of principal interest.

The observed improvement in film-cooling effectiveness for a curved coolant tube is sufficiently large in a practical range of blowing rates to warrant further investigation and consideration for turbine-blade designs incorporating the curvature feature.

The film-cooling performance of the looped coolant tube was inferior to both the straight and curved tubes at all blowing rates.

Lewis Research Center,
National Aeronautics and Space Administration,
Cleveland, Ohio, June 29, 1979,
505-04.

REFERENCES

1. Brinich, Paul F.; and Graham, Robert W.: Flow and Heat Transfer in a Curved Channel. NASA TN D-8464, 1977.
2. Graham, Robert W.; et al.: Heat Transfer and Fluid Mechanics. Nuclear Rocket Technology Conference, NASA SP-123, 1966, pp. 77-104.
3. Colladay, Raymond S.; Russell, Louis M.; and Lane, Jan M.: Streakline Flow Visualization of Discrete-Hole Film Cooling with Holes Inclined 30° to Surface. NASA TN D-8175, 1976.
4. Schlichting, Hermann (J. Kesten, transl.): Boundary Layer Theory. McGraw-Hill Book Co., Inc., 1955, p. 35.

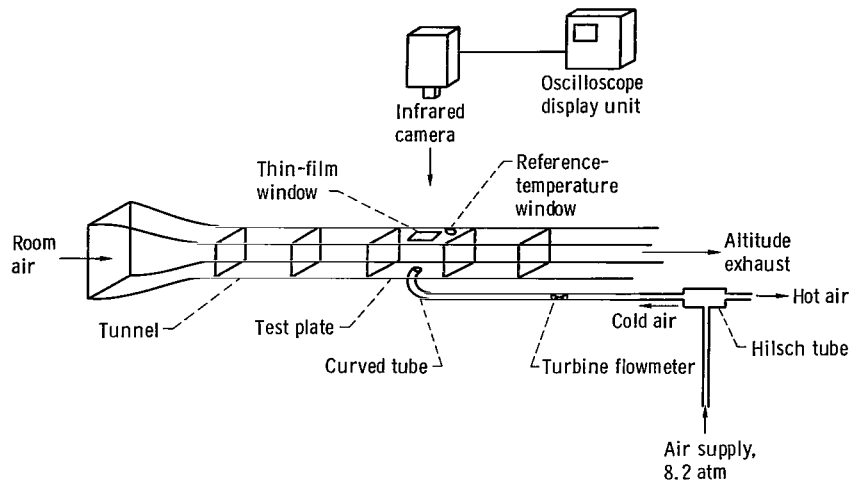


Figure 1. - Schematic of film-cooling rig.

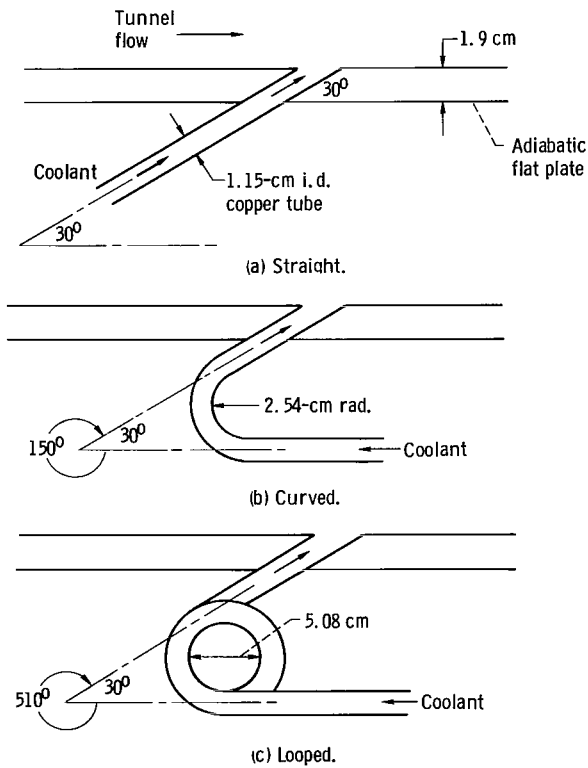


Figure 2. - Straight, curved and looped coolant-tube geometries.

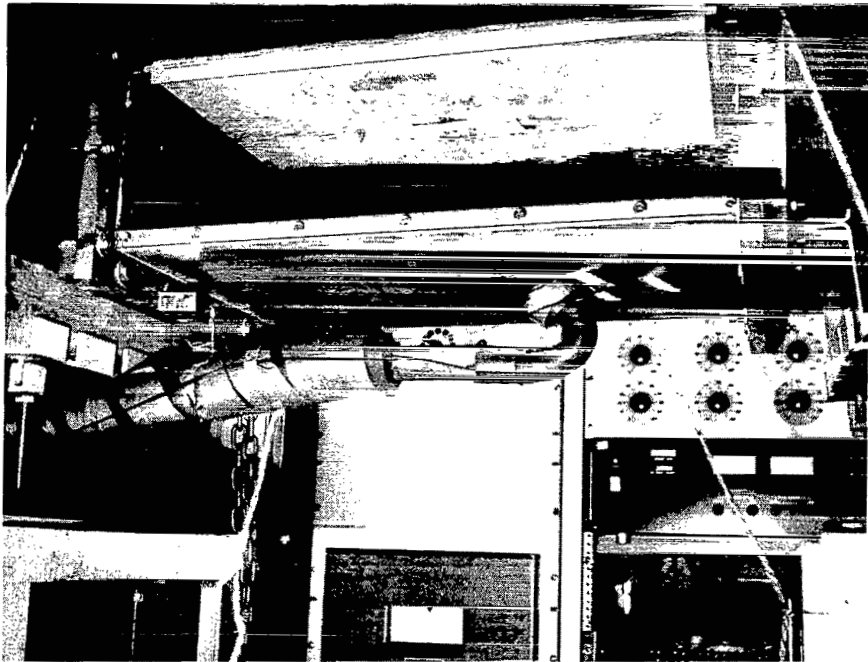
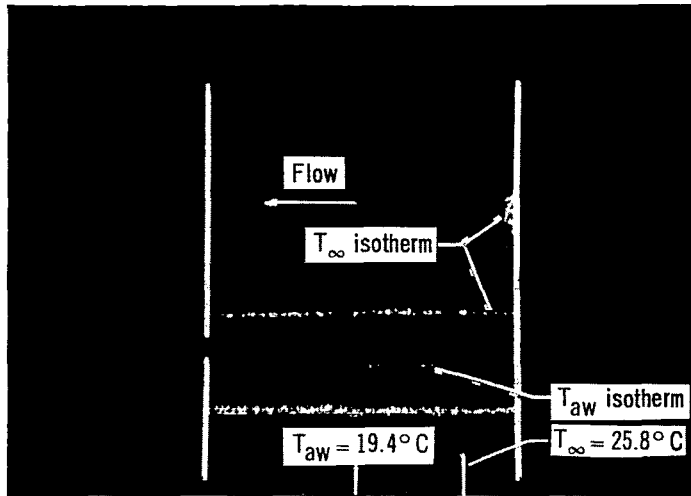
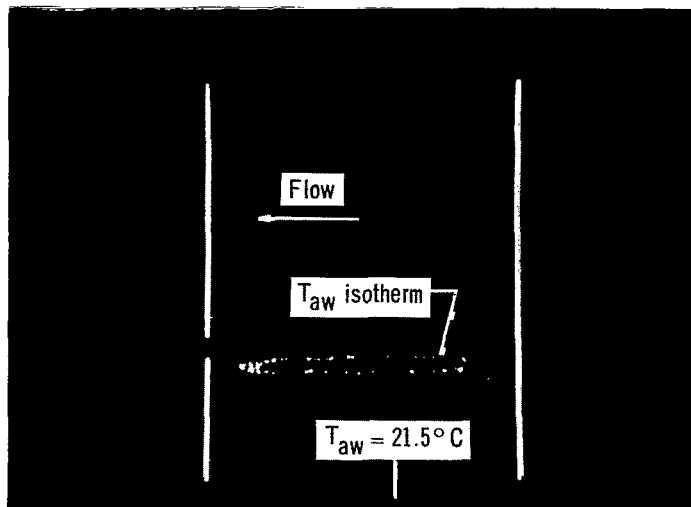


Figure 3. - Photograph of tunnel test section showing curved tube mated with flat plate.



(a) Wall temperature, 19.4°C .



(b) Wall temperature, 21.5°C .

Figure 4. - Photographs of isotherm traces.

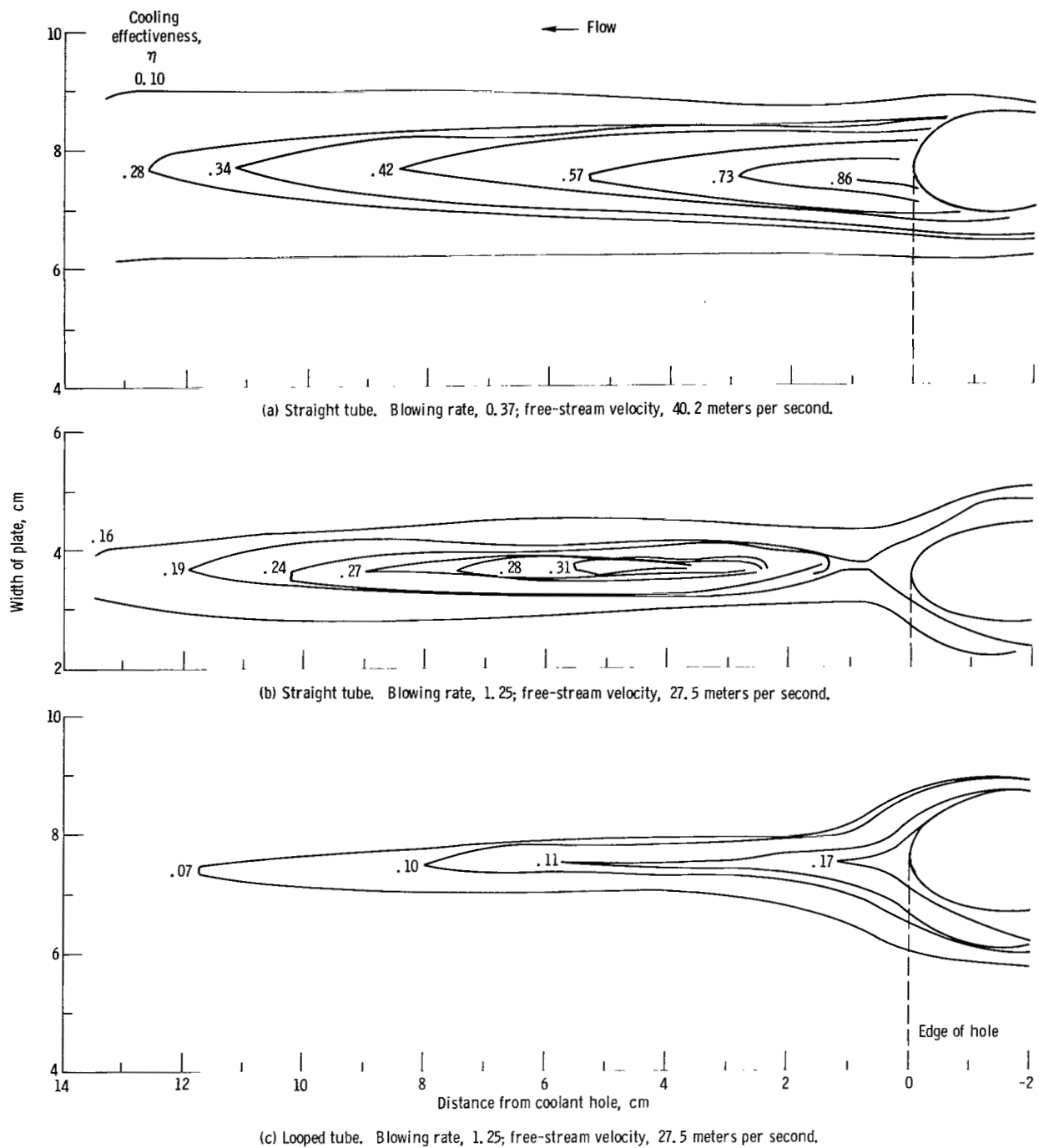


Figure 5. - Computer plots of actual-size isotherm traces. Coolant-tube injection angle, 30° .

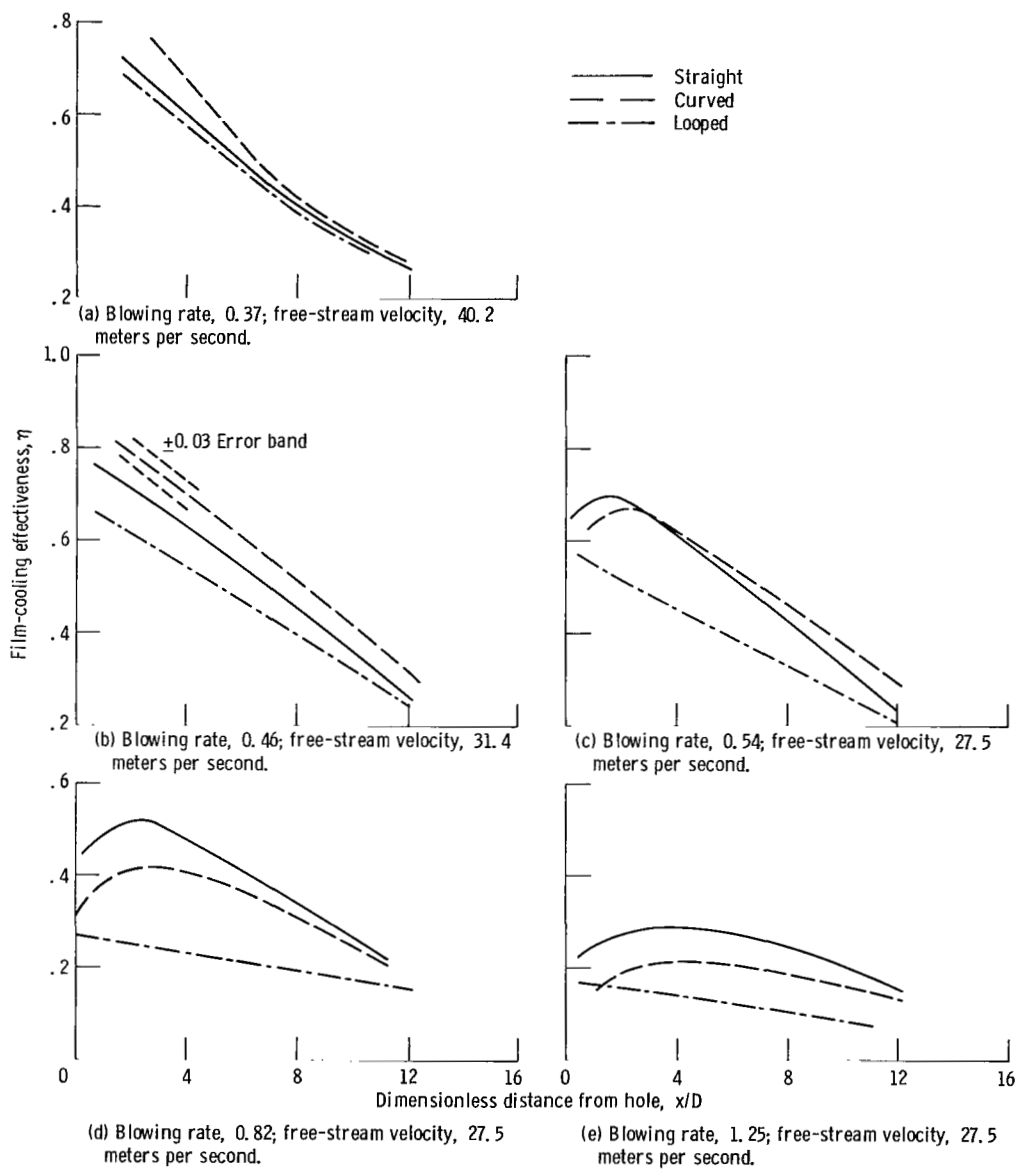


Figure 6. - Centerline effectiveness distributions for straight, curved, and looped coolant tubes. Injection angle, 30° .

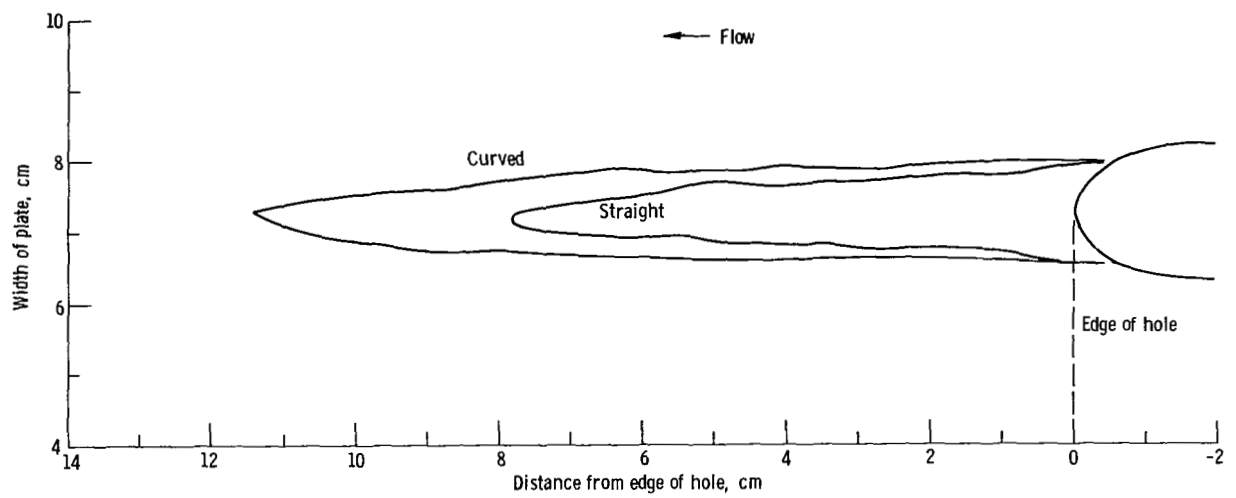


Figure 7. - Computer plot of actual size isotherm trace; comparison of straight and curved tubes. Cooling effectiveness, 0.46; blowing rate, 0.46; free-stream velocity, 31.4 meters per second.

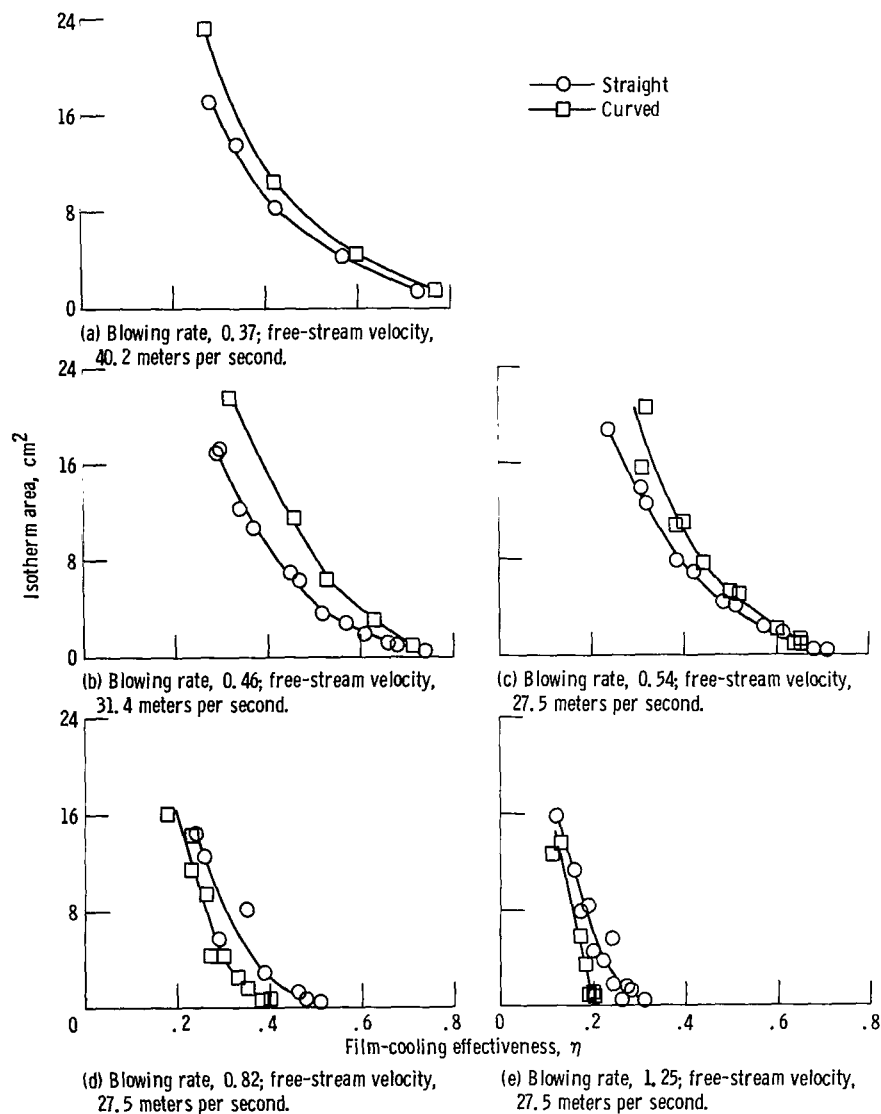


Figure 8. - Isotherm surface area coverage of straight and curved tubes. Coolant injection angle, 30°.

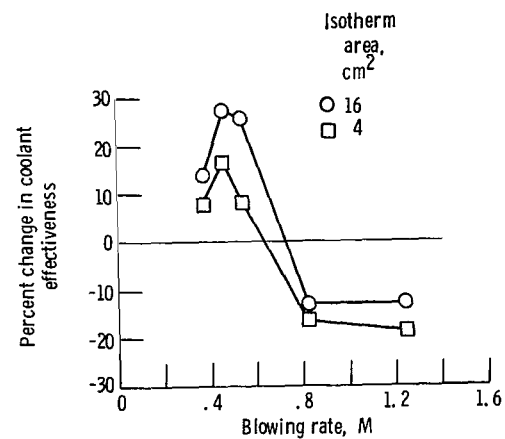


Figure 9. - Percent change in film-cooling effectiveness caused by curvature between 4 and 16 centimeters of coolant coverage.

1. Report No. NASA TP-1546		2. Government Accession No.		3. Recipient's Catalog No.	
4. Title and Subtitle INFLUENCE OF COOLANT TUBE CURVATURE ON FILM COOLING EFFECTIVENESS AS DETECTED BY INFRARED IMAGERY				5. Report Date November 1979	
				6. Performing Organization Code	
7. Author(s) S. Stephen Papell, Robert W. Graham, and Richard P. Cageao				8. Performing Organization Report No. E-066	
9. Performing Organization Name and Address National Aeronautics and Space Administration Lewis Research Center Cleveland, Ohio 44135				10. Work Unit No. 505-04	
				11. Contract or Grant No.	
12. Sponsoring Agency Name and Address National Aeronautics and Space Administration Washington, D.C. 20546				13. Type of Report and Period Covered Technical Paper	
				14. Sponsoring Agency Code	
15. Supplementary Notes					
16. Abstract <p>Reported herein are comparative thermal film-cooling footprints observed by infrared imagery from straight, curved, and looped coolant-tube geometries. It was hypothesized that the differences in secondary flow and in the turbulence structure of flow through these three tubes should influence the mixing properties between the coolant and the main stream. The coolant was injected across an adiabatic plate through a hole angled at 30° to the surface and in line with the free-stream flow. The data cover a range of blowing rates (mass flow per unit area of coolant divided by free stream flow) from 0.37 to 1.25. The average temperature difference between coolant and tunnel air was 25° C. Data comparisons confirmed that coolant-tube curvature significantly influences film-cooling effectiveness. At the blowing rates of 0.37 to 0.54, the curved coolant tube was more effective than the straight tube by as much as 16 to 27 percent. At the higher blowing rates of 0.82 and 1.25, the curved tube was less effective by as much as 13 to 19 percent. This reversal in data trend occurred at a blowing rate of about 0.70. The film-cooling performance of the looped tube was inferior to both straight and curved tubes at all blowing rates.</p>					
17. Key Words (Suggested by Author(s)) Gas turbine cooling Film cooling Heat transfer			18. Distribution Statement Unclassified - unlimited STAR Category 07		
19. Security Classif. (of this report) Unclassified		20. Security Classif. (of this page) Unclassified		21. No. of Pages 16	
				22. Price* A02	

National Aeronautics and
Space Administration

Washington, D.C.
20546

Official Business

Penalty for Private Use, \$300

SPECIAL FOURTH CLASS MAIL
BOOK

Postage and Fees Paid
National Aeronautics and
Space Administration
NASA-451



3 1 1U,A, 110179 S00903DS
DEPT OF THE AIR FORCE
AF WEAPONS LABORATORY
ATTN: TECHNICAL LIBRARY (SUL)
KIRTLAND AFB NM 87117

NASA

POSTMASTER: If Undeliverable (Section 158
Postal Manual) Do Not Return
